

IR Sensor-based Grasp Planner for the Pisa/IIT SoftHand

E. Luberto, G. Santaera, Y. Wu, M. Gabiccini

Abstract—This paper presents an approach to refine grasps for soft robotic hands in the presence of uncertainty. Once a pre-planned grasp, e.g. from a database, has been selected for execution to an object detected in a scene, an infrared sensor-informed grasp planner is run that essentially reduces uncertainties related to object shape and its pose in the environment. The proposed method implements a grasp location optimization algorithm that allows to minimize the distances between hand fingertips and the object by continuously controlling the wrist pose and the amount of hand closing. Experimental studies with Kuka-lwr arm and Pisa/IIT SoftHand illustrate the benefit of the developed technique and the improvement in the grasping performance with respect to the open-loop execution of grasps planned on the basis of prior visual cues only.

I. INTRODUCTION

The problem of autonomous robotic grasping has been in the focus of robotic research community for the past several decades [1], [2], [3]. Intelligent, proficient grasp planners have been developed that allow robotic hand to perform grasping tasks closely to humans. For ideal scenarios, where the object shape and location are perfectly known, and precise control of robotic hand can be achieved, pre-programmed autonomous grasping may be possible. To this end, most of the proposed planners [4], [5] rely on finding optimal fingertip placement on the object, while the surrounding environments are considered to be avoided as obstacles. However, these approaches are limited by their hand rigidity and fragility, and the manipulation strategies are very far from those a human would execute in real scenarios.

A real-world grasps are often associated to some uncertainties, the most typical ones being related to object recognition and localization. Usually, robots are equipped with vision sensors [6], [7], [8] to help reducing this uncertainty. However, a certain amount of uncertainty is usually unavoidable due to poor vision results, or incomplete view coverage of the sensor, etc. Other uncertainty may correspond to unexpected location of the object, where in this case, tactile/torque sensors are required to gain some additional information and to refine the object location from contacts [9], [10], [11]. Therefore, dexterous grasping of objects under uncertainty remains a difficult and unsolved problem in robotics.

E. Luberto, G. Santaera, Y. Wu are with Centro di Ricerca E. Piaggio, Universit di Pisa, Largo L. Lazzarino 1, 56122 Pisa, Italy. santaeragaspore@inwind.it, ema.1bt@hotmail.it, yier.wu@for.unipi.it

M. Gabiccini is with Dipartimento di Ingegneria Civile e Industriale (DICI), Largo Lucio Lazzarino 1, 56122 Pisa, with Centro di Ricerca E. Piaggio, Universit di Pisa, Largo L. Lazzarino 1, 56122 Pisa, and with Department of Advanced Robotics (ADVR), Italian Institute of Technology, Via Morego 30, 16163 Genova, Italy. m.gabiccini@ing.unipi.it



Fig. 1. Pisa/IIT SoftHand with IR Sensors

To better tackle the above described types of uncertainty, researchers have proposed the use of underactuated and/or soft hands [12], [13]. The design is simpler, easier to control and allows object contact with hand parts other than the fingertips, as well as to explore the surrounding environment in order to achieve precise and stable grasp. The robotic hand studied in this paper is the Pisa/IIT SoftHand [14], which has only one degree of actuation, and is continuously deformable in an infinity of possible shapes through interaction with objects and environment. Incipient grasp with this type of Softhand has been successfully achieved with a wide variety of everyday objects [15]. However, problems still remain when one or several above mentioned uncertainties occur during the execution of grasping tasks with novel objects.

The lack of exact knowledge of target object shape and location in the environment can be compensated by the use of sensor feedback. To further improve the quality and reliability of robotic grasping, different strategies have been proposed to enhance the sensing capabilities of robotic manipulators. Enhancement of long-range vision sensor is one of the solutions, such as in-hand object tracking, hand extraction for object reconstruction, etc. However in general, image acquisition and processing are quite slow for online reactive response. Another solution relies on tactile sensors, which have been employed in numerous tasks [16], [17], whereas they require premature contacts with the object and may cause significant object motion.

On the other hand, short-range infrared (IR) sensors are widely used in robotic applications thanks to their low-cost, fast response time and reduced sensitivity to the environment. In robotic grasping, IR sensors have been introduced during final grasp adjustments. In [18], the authors detect the

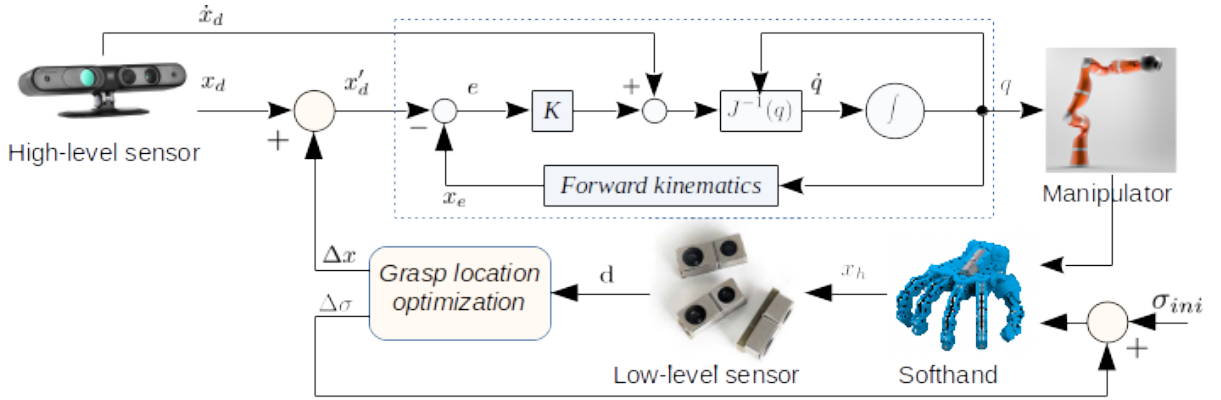


Fig. 2. Control Scheme of Sensor-based Grasping

orientation of an object surface using the IR sensors that fit inside the fingers. In [19], a shared-control algorithm has been proposed based on long-range vision sensor and infrared sensors for teleoperation-based grasping. In [20], robust grasping has been achieved using an IR Net-structure proximity sensor for objects with unknown position and attitude. However, these approaches have been developed for robotic hands with sensible rigidity and high degrees of actuation (4-8). Limited number of work address the problem of grasping refinement for compliant hands based on IR sensor measurements, which looks very promising here.

In this work, an approach to grasp refinement for the Pisa/IIT Softhand under uncertainty using IR sensors is presented. Based on sensor measurement feedback, the proposed algorithm allows to center the Softhand fingers around the object and wrap the hand around it in a uniform manner. It is effective, high-speed, does not cause premature object contact nor needs re-grasping strategies. It allows the robotic hand to perform online adjustments before final grasping.

To address the above mentioned problems, the remainder of the paper is organized as follows. Section II presents the problem of grasping with our Softhand. Section III describes the IR sensor working principle and the measurements is provided. In Section IV, an algorithm of grasp location refinement of the Softhand is presented. Section V contains the experimental results obtained for IR sensor-based grasp of novel objects using Kuka-lwr and Pisa/IIT Softhand. Finally, Section VI summarizes the main results and contributions of this paper.

II. PROBLEM STATEMENT

Despite the fact that contemporary vision systems are able to reconstruct fairly good 3D object models, which allows to considerably reduce the related uncertainties, it requires enormous time and manpower to build a point cloud library for each novel object, yet still incomplete to guarantee a stable final grasp. To reduce the time of visual acquisition and processing, we propose to use only the prior visual cue of an object, which leads the robot to a so-called

pre-grasp location. In order to ensure a stable final grasp, infrared sensors are mounted on the hand fingertips to gain some additional information about the hand location with respect to the object.



Fig. 3. Types of uncertainty during grasping

For the considered compliant hand, due to the peculiarities of its embedded soft and adaptive synergy [14], its configuration and exact fingertip locations are usually unknown after a grasp is executed. Therefore, the target object is approached by the hand via controlling wrist pose and hand closing. In order to improve the quality of grasp, we proposed to minimize the distances between hand fingertips by continuously controlling the wrist pose and the amount of hand closing based on IR sensor measurements. As the hand is closed in an informed manner, the proposed method allows to reduce the chance of significantly perturbing the object during the execution of the final grasp.

The overall control scheme of the robotic arm and hand is depicted in Fig. 2. The proposed grasp location optimization algorithm provides the correction values of wrist pose and hand closing at each time step. This control strategy allows to effectively improve the quality of grasp under uncertainty, such as visual incompleteness and/or coverage, unexpected change of object location, etc. (see Fig. 3).

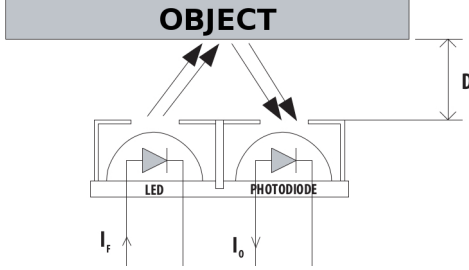


Fig. 4. IR Sensor working principle

III. SENSOR MEASUREMENTS

To measure the distances between hand fingertips and target object, we proposed to use infrared sensor. Its advantages include small size, low-cost, mechanical robustness and the simplicity to be managed with a micro-controller. The sensor consists of only one emitter and one receiver (See Fig. 4). The intensity of the transmitted infrared wave decreases according to the well known exponential law

$$E = E_0 e^{-\alpha x}, \quad (1)$$

where E_0 is the intensity of the original wave, x depends on the wave direction, and the parameter α varies with the material and increases with the wave frequency.

When the transmitted wave meets an object it splits in two, a refracted wave that spreads onto the object and a reflected one that comes back and meets the receiver. The intensity of these two waves depends on the reflection coefficient of the object material and on the angle at which the transmitted wave hits the object. The relation between the transmitted, refracted and reflected wave can be obtained using the Snell's law

$$k_1 \sin \theta_1 = k_2 \sin \theta_2, \quad (2)$$

where k_1, k_2 depend on the materials characteristics and θ_1, θ_2 are the angles between the wave travelling direction and the normal to the object surface. Usually the infrared wave is being transmitted and reflected through the same medium (the air, for instance), so $k_1 = k_2$ and, consequently, $\theta_1 = \theta_2$. Therefore, the desired distance between sensor and object can be obtained by measuring the intensities of the two waves.

However in most cases, it is hardly possible to know *a priori* the property of object material. To overcome this problem, one possible solution is to use the flight time, meaning that the sensor counts the time between the emission and reception of the infrared wave. Corresponding distance can be obtained as

$$d = \frac{vt_f}{2}, \quad (3)$$

where v is the wave propagation velocity, t_f is the flight time.

IV. GRASP REFINEMENT ALGORITHM

The IR sensors are mounted on the distal phalanges of all/a subset of the SoftHand fingers, according to the sensors' visibility w.r.t the object. Fig. 1 shows one of the possible arrangements of IR sensors, where only the thumb, index and ring finger are equipped. The sensor readings provide the distances between the phalanges and object within a range of about 60mm. It is assumed that all sensor measurements are collected in a vector $\mathbf{d} = [d_1, d_2, \dots, d_n]^T$, $d_i \geq 0$, where n indicates the number of sensors whose measurement is available (i.e. the sensor is seeing the object). Corresponding residual errors can be simply written as $r_i = d_i$. Since the goal is for the hand to approach the object in a homogeneous manner, the objective function of the optimization is defined as the root-mean-square errors of the residuals as follows

$$f = \sqrt{\sum_{i=1}^n d_i^2} \quad (4)$$

This objective is in fact a function of control input parameters $\underline{\mathbf{x}}$, who are the decision variables of the grasp location optimization problem. The size and nature of $\underline{\mathbf{x}}$ vary with the parameters of the control input (e.g, for joint position control, $\underline{\mathbf{x}} = [j_1, \dots, j_n]^T$, for wrist pose control, $\underline{\mathbf{x}} = [p_x, \dots, p_z, r_x, \dots, r_z]^T$). In this work, It is defined by the wrist pose together with the softhand closing, i.e. $\underline{\mathbf{x}} = [p_x, p_y, p_z, r_x, r_y, r_z, \sigma]^T$. Corresponding optimization problem can be formulated as

The residual vector $\underline{\mathbf{r}} = [r_1, \dots, r_n]^T$ obtained from sensor measurements is in fact a function of control input parameters $\underline{\mathbf{x}}$, which are the decision variables of the grasp location optimization problem. The size and nature of $\underline{\mathbf{x}}$ vary with the parameters of the control input (e.g, for joint position control, $\underline{\mathbf{x}} = [j_1, \dots, j_n]^T$, for wrist pose control, $\underline{\mathbf{x}} = [p_x, \dots, p_z, r_x, \dots, r_z]^T$). In this case, $\underline{\mathbf{x}}$ is defined by the arm wrist pose $(p_x, p_y, p_z; r_x, r_y, r_z)$ (6 DoF) together with the amount of hand closing, which is directly the synergy actuation (1 DoF), i.e. $\underline{\mathbf{x}} = [p_x, p_y, p_z; r_x, r_y, r_z; \sigma]^T$. The corresponding optimization problem can be formulated as

$$\min_{\underline{\mathbf{x}}} f(\underline{\mathbf{x}}), \quad \text{where } f(\underline{\mathbf{x}}) = \frac{1}{2} \underline{\mathbf{r}}(\underline{\mathbf{x}})^T \underline{\mathbf{r}}(\underline{\mathbf{x}}) \quad (5)$$

which is a *nonlinear* quadratic function w.r.t the decision variables $\underline{\mathbf{x}}$.

It is worth noting that, in the experimental setting, $f(\underline{\mathbf{x}})$ is only computable through execution of moves and measurement of sensor outputs. To reconcile the use of a gradient-based optimization algorithm with the intrinsic numerical nature of our $f(\underline{\mathbf{x}})$, we employ a Gauss-Newton strategy and form a linear approximation of the residual as follows

$$\underline{\mathbf{r}}(\underline{\mathbf{x}}) \simeq \underline{\mathbf{r}}_L(\Delta \underline{\mathbf{x}}) = \underline{\mathbf{r}}(\underline{\mathbf{x}}_k) + \mathbf{J}_r(\underline{\mathbf{x}}_k) \cdot \Delta \underline{\mathbf{x}}, \quad \text{where } \mathbf{J}_r = \frac{\partial \underline{\mathbf{r}}}{\partial \underline{\mathbf{x}}} \quad (6)$$

such that the optimal solution can be found step by step via corrections of the control inputs such that $\underline{\mathbf{r}} \rightarrow 0$ as k increases. In (6), $\underline{\mathbf{r}}(\underline{\mathbf{x}}_k)$ are the residuals measured at current

step k , \mathbf{J}_r is the Jacobian matrix of the residuals, and $\Delta\mathbf{x}$ is the correction displacements, which represent the next move. Here, \mathbf{J}_r is computed numerically based on the measurement data. In particular, each column can be approximated as

$$\mathbf{J}_r(:, j) \simeq \frac{\delta\mathbf{r}}{\delta\mathbf{x}_j} \quad (7)$$

where $\delta\mathbf{r}$ collects the changes in the measurements of residuals vector with respect to the change in each control input $\delta\mathbf{x}_j$. Using Eq. (5) and (6), one can obtain the solution of the quadratic approximation at k -th step

$$f_Q(\Delta\mathbf{x}_k) = \frac{1}{2}\mathbf{r}_L(\Delta\mathbf{x}_k)^T \mathbf{r}_L(\Delta\mathbf{x}_k) \quad (8)$$

of the original optimization problem (5) by seeking where $\frac{\partial f_Q(\Delta\mathbf{x}_k)}{\partial\Delta\mathbf{x}_k} = \mathbf{0}^T$, which yields

$$\Delta\mathbf{x}_k = -\mathbf{J}_r^+(\mathbf{x}_k) \mathbf{r}_k \quad (9)$$

Note that $\mathbf{J}_r^+ = (\mathbf{J}_r^T \mathbf{J}_r)^{-1} \mathbf{J}_r^T$ is the pseudo-inverse of the residual Jacobian. This allows us to update the subsequent hand location/configuration by adding the step as follows

$$\mathbf{x}_{k+1} = \mathbf{x}_k + \alpha\Delta\mathbf{x}_k \quad (10)$$

where $\alpha \in [0, 1]$ is proper scaling factor calibrated according to bounds on the robot and hand joint velocities.

Based on the above method for pre-grasp optimization, a detailed procedure is proposed which is summarized in Algorithm 1. It should be mentioned that the strategies for approaching and moving the end-effector in steps no. 4 and no. 5 seem ambiguous due to the fact that these strategies highly depends on the particular circumstance of the sensors arrangement and measurements. More details on this aspect will be provided in the Sec. V.

V. EXPERIMENTAL VALIDATION

To confirm the applicability of the proposed grasp refinement algorithm and to demonstrate its benefits from a practical perspective, this section presents the experimental setup and procedure, the sensor peculiarities, as well as the experimental results of in terms of grasping performances on a set of everyday objects.

A. Experiment setup and procedure

To perform the grasping tasks, the following experimental setup was used:

- A RGB-D sensor, Asus Xtion ProLive [21], for acquisition of the object point cloud (frontal view only);
- A 7-DoF robotic manipulator, Kuka Lightweight IV [22], for object manipulation (maximum payload 7 kg);
- A 19-DoF, 1-DoA robotic hand, Pisa/IIT SoftHand, for object grasping;
- Three short-range IR sensors, Avago HDSL9100, mounted on three hand fingers (thumb, index and ring) for distance measurements;

Algorithm 1: Pre-Grasp Optimization

- 1: Acquiring object shape and location from a prior visual cue and obtain a pre-grasp location for the robotic arm;
 - 2: Moving the arm to the obtained location and bringing the grasping end-effector to a pre-grasp configuration;
 - 3: Checking the sensor measurements:
 if All sensors have no measurements on the object then
 Goto Step no. 4;
 if At least one sensor has measurement on the object then
 Goto Step no. 5;
 if All sensors have measurements on the object then
 Goto Step no. 6;
- 4: Approaching the grasping end-effector to the object and returning to step no. 3;
 - 5: Moving the grasping end-effector around the object according to particular strategy (depending on the sensors measurements), returning to step no. 3;
 - 6: Moving the grasping end-effector by sequentially changing each parameter of the control input $\delta\mathbf{x}$, while obtaining the differences in residual vector $\delta\mathbf{r}$ based on sensor measurements and return the end-effector to its previous state;
 - 7: Computing the residual Jacobian matrix using Eq. (7);
 - 8: Computing the corrections $\Delta\mathbf{x}$ for the succeeding step using Eq.(9);
 - 9: Moving and closing the grasping end-effector following Eq. (10), and reading the IR sensor measurements;
 - 10: Computing the objective function f using the new measurements:
 if $f > \text{threshold}$ then
 Goto Step 6;
 else
 Grasp the Object!
-

- A table and a set of three selected everyday objects.

Assuming that the vision sensor captures the object frontal view only, the grasp experiments are meant to evaluate the performance of the infrared sensor-based pre-grasp optimization in two different scenarios : (i) nominal object pose: the object is in the nominal pose given by the vision sensor; (ii) perturbed object pose: the object pose is different w.r.t. to estimated provided by the vision sensor. In case (i), all objects are assumed to be grasped at their predefined positions on the table. For objects that do not possess any axis of symmetry, the grasping experiments are performed with the object in two different orientations. For each object and each orientation, experiments are repeated three times. In case (ii), the same protocol of case (i) is repeated, except that objects are slightly moved away from their nominal positions (in translations and/or in orientation, depending on the symmetrical properties of corresponding object).

For comparison, grasping experiments are carried out both with and without applying the IR sensor-based optimization

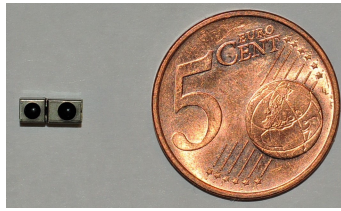


Fig. 5. Avago HDSL9100 Infrared Sensors

algorithm proposed. To demonstrate the advantages of our method, the analysis of grasping performances is presented in the following subsections, in terms of successful grasp rate. Then, the evolution of measured distances and of the wrist poses is presented to evaluate the converge behavior of the underlying optimization process.

B. Sensor features and measured outputs

In this work, the Avago HDSL9100 Infrared Sensor [23] (see Fig. 5) is selected due to its small size ($7 \times 3 \times 2.5$ mm), which fits the fingertips of Pisa/IIT SoftHand and provides a suitable operative range (4-65 mm) for the distance measurements. However, due to the small size of the sensor, a conditioning circuit is required to properly scale the sensor inputs and outputs. It goes without saying that the sensor operative range depends on the circuit components: here, they are tuned to obtain the maximum distance.

Another issue is related to the reciprocal of the sensors once placed on the fingerpads of the SoftHand. In our experiment, three IR sensors are used which are mounted on the thumb, index and ring fingers (see Fig. 1). This arrangement may cause some disturbances during the measurements: for instance, the light emitted by one sensor could be misread by another one. To overcome this problem, the conditioning circuit is designed to activate only one sensor at a time in a cyclic fashion.

The schematic of the conditioning circuit is illustrated in Fig. 6, where each sensor is activated by a square wave (D_o), and its output is read by an analog-digital converter (ADC). The physical output of the sensor is an electric voltage, which is proportional to the intensity of the reflected wave acquired by the receiver. Therefore, the higher the output voltage, the closer is the sensor to the object. The ADC returns the output voltage in a digital value in bits (or ticks), according to its resolution (12 bits on 5 Volt for the embedded microcontroller PSoC).

To simplify the design of conditioning circuit, instead of counting the sensor flight time (see Section III), which need a dedicated electronics stage, we use directly the output value of the ADC. In principle, the proposed algorithm, step by step along the local gradient, aims to reduce the mean squared distance between the object and the robot end-effector. It moves the end-effector of the robot and concurrently measures the distances, to understand which movements allows for a reduction in the overall distance. Summing up, to work properly the algorithm has not to need to know the exact value of distances in millimeters, but it is

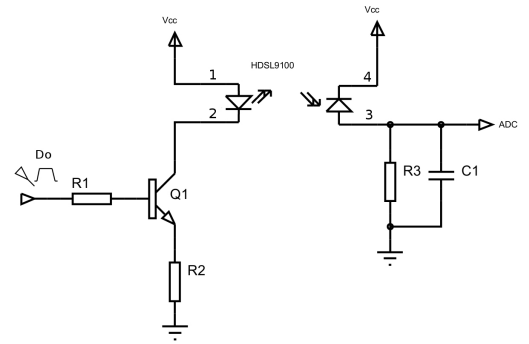


Fig. 6. Conditioning Circuit Schematic of IR Sensors

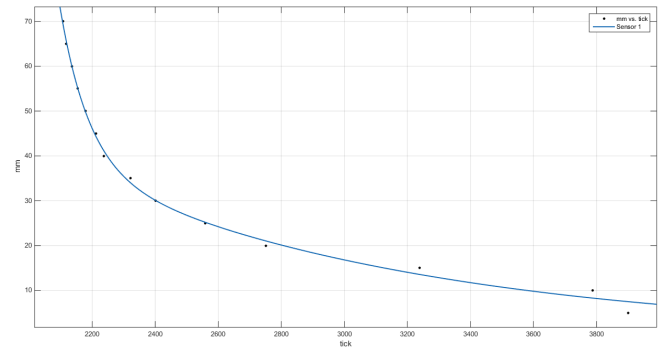


Fig. 7. Characterization Curve of One IR Sensor

enough only an evaluation of these ones. A good estimation of the distances by the output values of the analog-digital converter can be obtained using a characterization curve, which is given by the interpolation of some experimental measurements on a sample object. In the case of objects with reflection characteristics very different from the sample one, it could be needed to compute again the characterization curve. So this design choice allows to reduce the complexity of the conditioning circuit, but does not give accurate informations about the distances. The characterization curve of the sample object, used in this work, is depicted in Fig. 7 and it is obtained by the following equation.

$$y = ae^{bx} + ce^{dx}, \quad (11)$$

where y is the desired distance, x is ADC output, and the parameters a, b, c, d can slightly vary from one sensor to another due to the tolerances of conditioning circuit components.

C. Sensor measurements checks

In Algorithm (1), before computing the residual Jacobian matrix, one has to ensure that all sensors are in their operative range. The check on the IR sensors, Step no. 3, depends on the specific configuration of the sensor installed. If at least one sensors measures a distance higher than 60 mm the current SoftHand position is changed in order to hook some parts of the object. In the figures 8 and 9 are shown the strategies used to move a left SoftHand to explore the scenario.

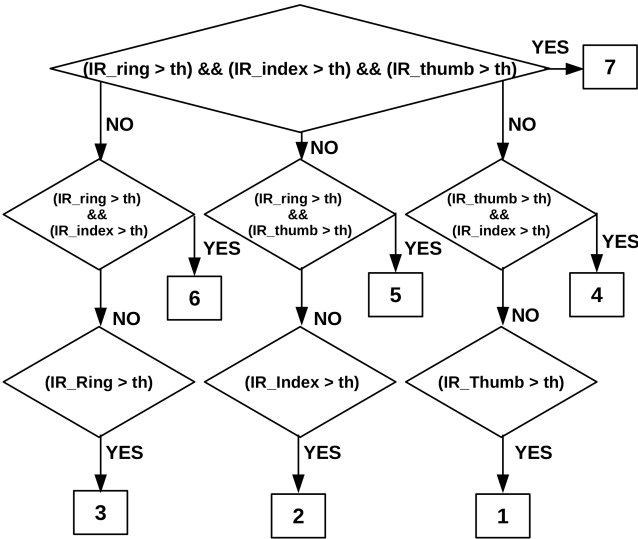


Fig. 8. Definitions of all possible cases in which the sensors are over the operative range, th is setted on 60mm.

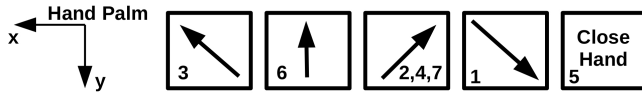


Fig. 9. Summary of the directions in which the left SoftHand has to be moved according to the cases previously defined

In Fig. 9, x and y are the directions in which the SoftHand frame $\{\text{SH}\}$ moves with respect to the world frame $\{\text{world}\}$ (see Fig. 10).

D. Grasp results

The results of the grasping experiments are given in Table I, where the number of successful grasps are provided for each object. Comparison are made for grasping with and without the proposed algorithm.

Object and reference pose	Nominal Pose (\mathfrak{N})		Perturbed Pose (\mathfrak{P})	
	IR-guided	Blind	IR-guided	Blind
Cylinder	2/3	0/3	3/3	0/3
Baby cup, pose (a)	1/3	0/3	1/3	0/3
Baby cup, pose (b)	3/3	1/3	2/3	0/3
Paper box, pose (a)	2/3	0/3	1/3	0/3
Paper box, pose (b)	2/3	1/3	1/3	0/3
Total	10/15	2/15	8/15	0/15

TABLE I

SUCCESSFUL GRASPS FOR DIFFERENT OBJECTS IN NOMINAL (\mathfrak{N}) AND PERTURBED (\mathfrak{P}) POSE, WHEN EMPLOYING IR-GUIDED OR BLIND GRASP STRATEGIES.

This table shows the successful grasp attempts with respect to the repetitions performed. Each row refers to an object and a reference pose. The first two columns report the successful grasps in the nominal (\mathfrak{N}) object pose, for IR-guided and Blind grasps, respectively. The third and fourth columns report the successful grasps in the perturbed (\mathfrak{P}) object pose, for IR-guided and Blind grasps, respectively.

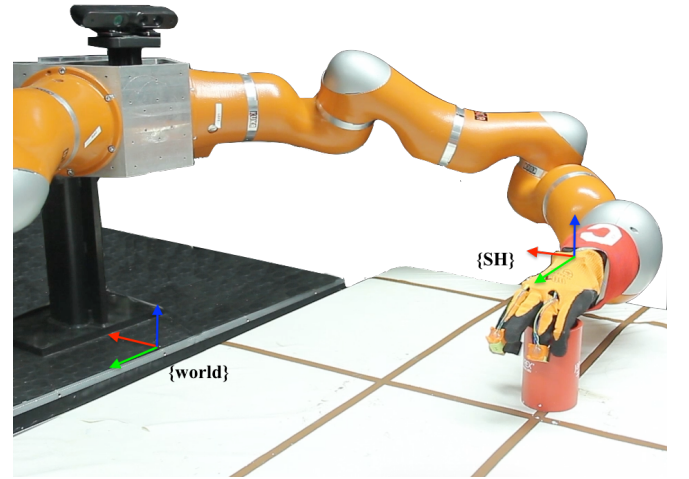


Fig. 10. Scenario with the SoftHand frame $\{\text{SH}\}$ and world frame $\{\text{world}\}$

Clearly, using only the prior visual cue of the object and performing the grasp task at corresponding pre-grasp location, the number of successful grasps is very low. In the case of perturbed grasp, when the object pose are deliberately moved, the successful grasp reduced to none. Applying the proposed sensor-based grasp planner, the successful rate have been considerably increased by 54% and 53% in case of grasp at nominal and perturbed pose, respectively.

Fig. 12 shows some of the sensor measurements during the execution of grasps at nominal object poses. The red line describes the minimization of the root-mean-distance achieved by using the proposed IR sensor-based grasp planner. The other three curves report the measured distances from the index, thumb and ring fingertips at each time step. Fig. 14 illustrates the same contents for grasps at perturbed object poses.

In most of the performed grasp tasks, measurements of the index fingertips show that it is always further from the object than the other two fingers, whereas the thumb and ring are well centered with respect to the object. This is due to the particular softhand synergy, each finger closes differently driven by the same amount of hand closing. In this case, the index has relatively small amount of closure comparing to the other two fingers. However in practical grasp, such hand configuration can guarantee a stable grasp for most objects.

Table II present the sensor measurements of distances between the hand fingertips and different objects, at the last step where the IR-guided or Blind grasp planner was applied. From this table, it is clear that the proposed sensor-informed grasp planner essentially reduced the distances from the softhand to the object comparing to a pre-grasp hand configuration. In most of the performed grasping tasks, a stable grasp has been achieved at a distance about three to four centimeters from the object.

VI. CONCLUSIONS

In this paper we presented an effective and efficient method to refine the final grasping pose of a soft robotic hand with respect an object, using low-cost IR sensors. The

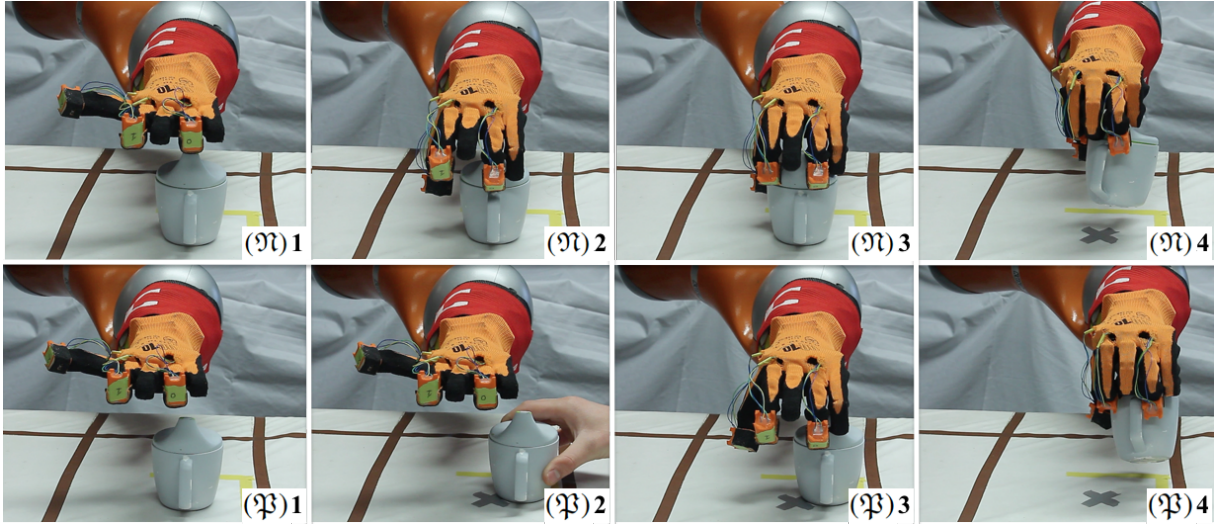


Fig. 11.

Sequences of the IR sensor-based grasp planner in Nominal (\mathfrak{M}) and Perturbed ($\mathfrak{M}\bar{\cdot}$) pose
 (\mathfrak{M}) - 1 init SoftHand position, 2 and 3 two subsequent step of the algorithm, 4 final grasp.
 $(\mathfrak{M}\bar{\cdot})$ - 1 init SoftHand position, 2 object perturbed and start CheckIR phase, 3 IR sensor-based grasp planner, 4 final grasp.

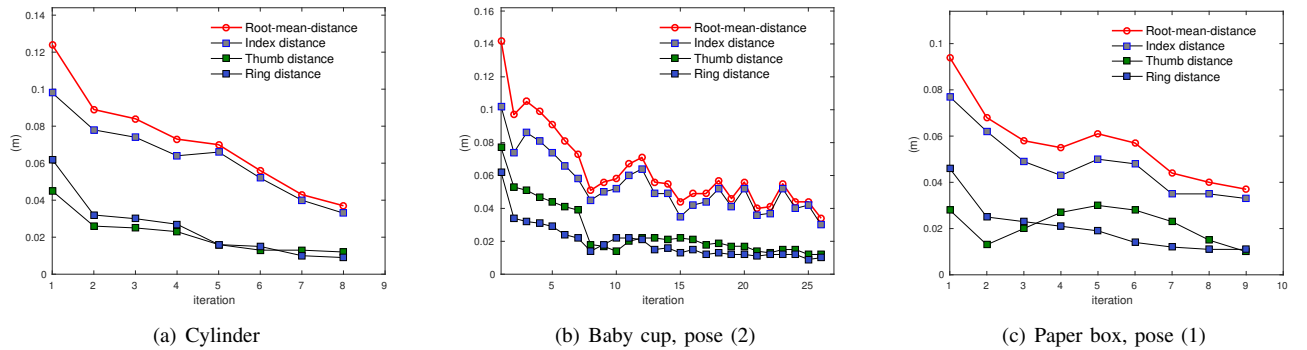


Fig. 12. Sensor measurements for grasping in nominal pose (\mathfrak{M})

Object	Nominal Pose (\mathfrak{M})		Perturbed Pose ($\mathfrak{M}\bar{\cdot}$)	
	Blind	IR-guided	Blind	IR-guided
Cylinder	0.124	0.037	0.119	0.028
Baby cup	0.142	0.034	0.139	0.028
Paper box	0.094	0.037	0.085	0.025

TABLE II

DISTANCE MEASUREMENTS OF HAND FINGERTIPS IN NOMINAL AND PERTURBED POSE, AT THE LAST STEP OF IR-GUIDED AND BLIND GRASP PLAN [M]

problem has been framed as a nonlinear optimization one, where the mean distance between the sensorized fingerpads and the object is minimized. An algorithm has been proposed which allows to apply Gauss-Newton steps to command the hand pose with the goal of centering the hand around an object, whose location and shape have been acquired through vision and can be altered significantly. The algorithm was tested on a Kuka-LWR arm and Pisa/IIT SoftHand by performing grasp tasks in the presence of uncertainty in the

object pose. The outcomes showed the effectiveness of the proposed method and essential improvement in the grasping performance with respect to a blind grasping strategy. Future work will address the full use of the IR sensors on all fingers, taking into account the adaptive synergy of the softhand, to exploit the capabilities of the sensorized softhand for perception of unstructured environments.

VII. ACKNOWLEDGMENTS

This work is supported by the grant no. 600918 PAC-MAN - Probabilistic and Compositional Representations of Object for Robotic Manipulation - within the FP7-ICT- 2011-9, and under grant agreement no. 645599 SoMa - Soft-bodied intelligence for Manipulation, within the H2020-ICT-2014-1.

REFERENCES

- [1] A. Bicchi and V. Kumar, "Robotic grasping and contact: a review," in *Robotics and Automation, 2000. Proceedings. ICRA '00. IEEE International Conference on*, vol. 1, 2000, pp. 348–353.

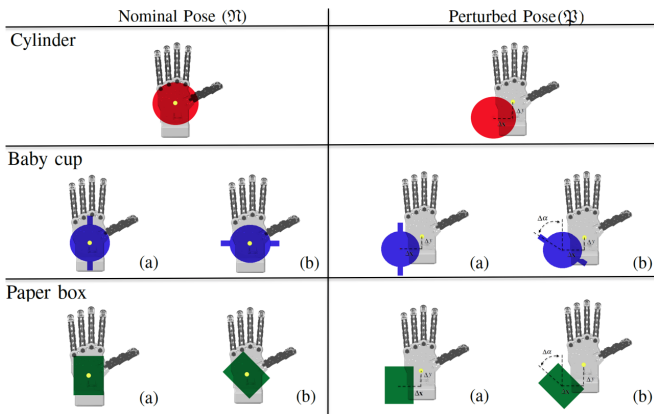


Fig. 13. Grasping experiments in Nominal (\mathfrak{M}) and Perturbed (\mathfrak{P}) pose

- [2] A. M. Okamura, N. Smaby, and M. R. Cutkosky, "An overview of dexterous manipulation," in *Robotics and Automation, 2000. Proceedings. ICRA'00. IEEE International Conference on*, vol. 1. IEEE, 2000, pp. 255–262.
- [3] C. C. Kemp, A. Edsinger, and E. Torres-Jara, "Challenges for robot manipulation in human environments," *IEEE Robotics and Automation Magazine*, vol. 14, no. 1, p. 20, 2007.
- [4] R. Diankov and J. Kuffner, "Openrave: A planning architecture for autonomous robotics," *Robotics Institute, Pittsburgh, PA, Tech. Rep. CMU-RI-TR-08-34*, vol. 79, 2008.
- [5] A. Miller and P. Allen, "Graspit! a versatile simulator for robotic grasping," *Robotics Automation Magazine, IEEE*, vol. 11, no. 4, pp. 110–122, 2004.
- [6] C. Kemp, C. Anderson, H. Nguyen, A. Trevor, and Z. Xu, "A point-and-click interface for the real world: Laser designation of objects for mobile manipulation," in *Human-Robot Interaction (HRI), 2008 3rd ACM/IEEE International Conference on*, Mar. 2008, pp. 241–248.
- [7] A. Saxena, J. Driemeyer, and A. Y. Ng, "Robotic grasping of novel objects using vision," *The International Journal of Robotics Research*, vol. 27, no. 2, pp. 157–173, 2008.
- [8] B. Wang, L. Jiang, J. Li, and H. Cai, "Grasping unknown objects based on 3d model reconstruction," in *Advanced Intelligent Mechatronics. Proceedings, 2005 IEEE/ASME International Conference on*, Jul. 2005, pp. 461–466.
- [9] J. Tegin and J. Wikander, "Tactile sensing in intelligent robotic manipulation-a review," *Industrial Robot: An International Journal*, vol. 32, no. 1, pp. 64–70, 2005.
- [10] L. Natale and E. Torres-Jara, "A sensitive approach to grasping," in *Proceedings of the sixth international workshop on epigenetic robotics*. Citeseer, 2006, pp. 87–94.
- [11] J. Romano, K. Hsiao, G. Niemeyer, S. Chitta, and K. Kuchenbecker, "Human-inspired robotic grasp control with tactile sensing," *Robotics, IEEE Transactions on*, vol. 27, no. 6, pp. 1067–1079, Dec. 2011.
- [12] L. U. Odhner, L. P. Jentoft, M. R. Claffee, N. Corson, Y. Tenzer, R. R. Ma, M. Buehler, R. Kohout, R. D. Howe, and A. M. Dollar, "A compliant, underactuated hand for robust manipulation," *The International Journal of Robotics Research*, vol. 33, no. 5, pp. 736–752, 2014.
- [13] R. Deimel and O. Brock, "A novel type of compliant and underactuated robotic hand for dexterous grasping," *The International Journal of Robotics Research*, p. 0278364915592961, 2015.
- [14] M. G. Catalano, G. Grioli, E. Farnioli, A. Serio, C. Piazza, and A. Bicchi, "Adaptive synergies for the design and control of the pisa/iit soft-hand," *The International Journal of Robotics Research*, vol. 33, no. 5, pp. 768–782, 2014.
- [15] M. Bonilla, E. Farnioli, C. Piazza, M. Catalano, G. Grioli, M. Garabini, M. Gabiccini, and A. Bicchi, "Grasping with soft hands," in *Humanoid Robots (Humanoids), 2014 14th IEEE-RAS International Conference on*. IEEE, 2014, pp. 581–587.
- [16] D. Gunji, Y. Mizoguchi, S. Teshigawara, A. Ming, A. Namiki, M. Ishikawaand, and M. Shimojo, "Grasping force control of multi-fingered robot hand based on slip detection using tactile sensor," in *Robotics and Automation, 2008. ICRA 2008. IEEE International Conference on*, May 2008, pp. 2605–2610.
- [17] J. Felip and A. Morales, "Robust sensor-based grasp primitive for a three-finger robot hand," in *Intelligent Robots and Systems, 2009. IROS 2009. IEEE/RSJ International Conference on*. IEEE, 2009, pp. 1811–1816.
- [18] K. Hsiao, P. Nangeroni, M. Huber, A. Saxena, and A. Ng, "Reactive grasping using optical proximity sensors," in *Robotics and Automation, 2009. ICRA '09. IEEE International Conference on*, May 2009, pp. 2098–2105.
- [19] N. Chen, K. P. Tee, and C.-M. Chew, "Teleoperation grasp assistance using infra-red sensor array," *Robotica*, vol. 33, no. 04, pp. 986–1002, 2015.
- [20] S. Ye, K. Suzuki, Y. Suzuki, M. Ishikawa, and M. Shimojo, "Robust robotic grasping using IR net-structure proximity sensor to handle objects with unknown position and attitude," in *Robotics and Automation (ICRA), 2013 IEEE International Conference on*, May 2013, pp. 3271–3278.
- [21] "Asus xtion pro live home page," online; accessed 22-February-2016. [Online]. Available: https://www.asus.com/3D-Sensor/Xtion_PRO_LIVE/
- [22] R. Bischoff, J. Kurth, G. Schreiber, R. Koeppe, A. Albu-Schffer, A. Beyer, O. Eiberger, S. Haddadin, A. Stemmer, G. Grunwald, and G. Hirzinger, "The kuka-dlr lightweight robot arm - a new reference platform for robotics research and manufacturing," in *Robotics (ISR), 2010 41st International Symposium on and 2010 6th German Conference on Robotics (ROBOTIK)*. IEEE, 2010.
- [23] "Hds9100 datasheet page," online; accessed 18-February-2016. [Online]. Available: <http://www.avagotech.com/docs/AV02-2259EN>

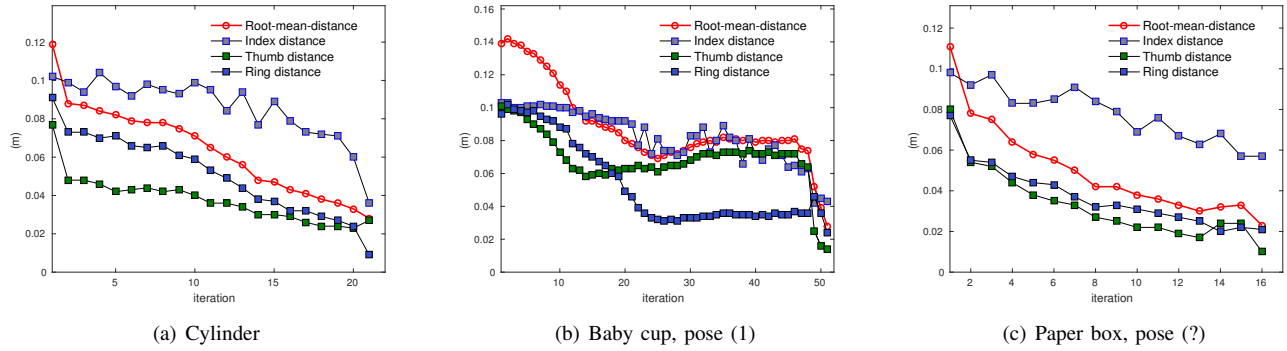


Fig. 14. Sensor measurements for grasping in perturbed pose (\mathfrak{P})